Sample Size Estimation of Transfer Learning for Colorectal Cancer Detection

Ruihao Luo[1,2][a], Shuxia Guo[1,2][b] and Thomas Bocklitz[1,2,3][c]
[1]*Leibniz Institute of Photonic Technology, Albert-Einstein-Straße 9, 07745 Jena, Germany*
[2]*Institute of Physical Chemistry and Abbe Center of Photonics, Friedrich-Schiller-Universität Jena, Helmholtzweg 4, 07743 Jena, Germany*
[3]*Institute of Computer Science, Faculty of Mathematics, Physics & Computer Science, Universität Bayreuth, Universitätsstraße 30, 95447 Bayreuth, Germany*

Keywords: Transfer Learning, Sample Size Estimation, Colorectal Cancer.

Abstract: Nowadays, deep learning has been widely implemented into biomedical applications, but it is problematic to acquire large annotated medical datasets to train the models. As a technique for reusing knowledge obtained from one domain in another domain, transfer learning can be used with only small datasets. Despite of some current research about model transfer methods for medical images, it is still unclear how sample size influences the model performance. Therefore, this study focuses on the estimation of required sample size for a satisfactory performance, and also compares transfer methods with only 200 images randomly chosen from a colorectal cancer dataset. Firstly, based on a K-fold cross-validation, the balanced accuracies of 3 transfer learning networks (DenseNet121, InceptionV3 and MobileNetV2) were generated, and each network used 3 model transfer methods, respectively. Afterwards, by curve fitting with inverse power law, their learning curves were plotted. Furthermore, the estimation of required sample size as well as the prediction of final performance were calculated for each model. In addition, to investigate how many images are needed for curve fitting, the maximum number of images also changed from 200 to smaller numbers. As a result, it is shown that there is a trade-off between predicted final performance and estimated sample size, and suggested model transfer methods for large datasets do not automatically apply to small datasets. For small datasets, complicated networks are not recommended despite of high final performance, and simple transfer learning methods are more feasible for biomedical applications.

1 INTRODUCTION

As a popular machine learning technique, deep learning has been widely applied into the field of biomedical research (Lecun et al., 2015). For example, Cheung et al. developed a deep learning model for Alzheimer's disease detection (Cheung et al., 2022); Foersch et al. used deep learning for colorectal cancer therapy (Foersch et al., 2023); Placido et al. predicted pancreatic cancer by deep learning (Placido et al., 2023); Narayan et al. built up an Enhance-Net to boost performance on real-time medical images (Narayan et al., 2023); Wang et al. created a deep learning toolkit called PyMIC for annotation-efficient medical image segmentation (Wang et al., 2023).

However, it is practically difficult to obtain large amounts of annotated medical data to train deep learning models due to legal restrictions, ethical reasons and workload. Therefore, the model performance is limited (Rajpurkar et al., 2022). Because of the ability of reusing knowledge from different domains, transfer learning has prevailed in this area (Zhuang et al., 2021). In the recent study of Luo and Bocklitz, different model transfer methods were compared on a colorectal cancer dataset, and some of them demonstrated satisfactory performance (Luo & Bocklitz, 2023). For instance, using pre-

[a] https://orcid.org/0000-0002-8291-4927
[b] https://orcid.org/0000-0001-8237-8936
[c] https://orcid.org/0000-0003-2778-6624

Luo, R., Guo, S. and Bocklitz, T.
Sample Size Estimation of Transfer Learning for Colorectal Cancer Detection.
DOI: 10.5220/0012449500003654

In *Proceedings of the 13th International Conference on Pattern Recognition Applications and Methods (ICPRAM 2024)*, pages 841-851
ISBN: 978-989-758-684-2; ISSN: 2184-4313

trained transfer learning networks with added convolutional layers could achieve validation accuracies above 0.95 on a dataset with more than 9,000 images regardless of computational complexity. Besides, Soekhoe and Putten revealed that dataset size influences classification accuracy of transfer learning with general images (Soekhoe & Putten, 2016); Samala et al. studied the effects of training sample size on multi-stage transfer learning for digital breast tomosynthesis (Samala et al., 2019); Zhu et al. investigated from plastics manufacturing images that training sample size could influence classification performance for transfer learning models (Zhu et al., 2021).

Despite of current research about classification models as well as model transfer methods for biomedical images, how sample size influences the model performance remains to be investigated further. So, this study focuses on the estimation of required sample size for an acceptable performance, and also compares model transfer methods with only 200 limited images randomly chosen from a colorectal cancer dataset (Kather et al., 2019).

2 TRANSFER LEARNING FOR BIOMEDICAL IMAGES

Although data scarcity poses a real threat in the field of biomedicine, transfer learning models have already showed the efficacy by reusing the knowledge gained from other domains (Kim et al., 2022). Based on the research of Yu et al., transfer learning models are already applied for biomedical image analysis of brain, lung, breast cancer, kidney diseases as well as other diseases (Yu et al., 2022). And these transfer learning models mostly reuse the knowledge obtained from ImageNet, which is a large-scale visual database containing more than 14 million images (Russakovsky et al., 2015).

In this study, 3 transfer learning base models were chosen based on their popularity (Morid et al., 2021): DenseNet121 (Huang et al., 2017), InceptionV3 (Szegedy et al., 2016) and MobileNetV2 (Sandler et al., 2018). DenseNet121 has a 7*7 convolutional layer, 58 3*3 convolutional layers, 61 1*1 convolutional layers, 4 average pooling layers and a fully-connected layer at the end. InceptionV3 is made up of 42 layers, which contains 3 inception modules, 6 convolutional layers as well as final pooling and fully-connected layers. MobileNetV2 consists of the initial fully convolution layer with 32 filters, followed by 19 inverted residual bottleneck layers. There are different options of model transfer methods for these transfer learning models, and it has been studied that adding convolutional layers (‘add’) outperforms simply using the original networks (‘ori’) or fine-tuning some last layers (‘ft’) (Luo & Bocklitz, 2023). However, this study was only conducted with enough images, the model performance still needs to be checked with very limited images.

Therefore, with maximal sample size of 200, containing both microsatellite unstable or hypermutated (MSIMUT) and microsatellite stable (MSS) images randomly selected with equal amounts (Kather et al., 2019), 3 model transfer methods (‘ori’, ‘ft’ and ‘add’) as well as 3 base models (DenseNet121, InceptionV3 and MobileNetV2) were analysed in this study without data augmentation. Notably, ‘ft1’, ‘ft2’ and ‘ft3’ refer to fine-tuning the last 1, 2 or 3 convolutional layers, respectively; likewise, ‘add1’, ‘add2’, ‘add3’ refer to adding 1, 2, or 3 convolutional layers at the end, but before the SoftMax layer, respectively. The study workflow is shown in Figure 1.

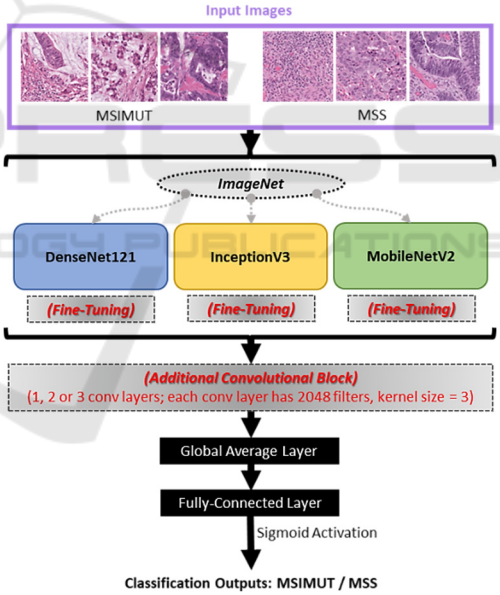

Figure 1: Transfer learning model architectures.

3 LEARNING CURVE GENERATION BASED ON K-FOLD CROSS VALIDATION

By separating a dataset into a training part and a validation part, K-fold cross-validation is commonly used as a method against over-fitting or under-fitting, and it can also be implemented to evaluate the model

generalisation ability (Kohavi, 1995). In this study, firstly image subsets were generated by randomly sampling from a colorectal cancer dataset. Afterwards, for each image subset (sample), it was sent to an external K-fold cross-validation loop. Inside the loop, the training part was used for model training, and the validation part was used for model validation. Finally, the model performance was evaluated based on validation balanced accuracies.

In machine learning, a usual method to assess classification performance as a function of sample size is to build empirical scaling models called learning curves (Cortes et al., 1994). Thus, with sample sizes varying from 20 to 200, a learning curve for each trained model was generated in this study. The overall dataflow of learning curve generation based on K-fold cross-validation is demonstrated in Figure 2.

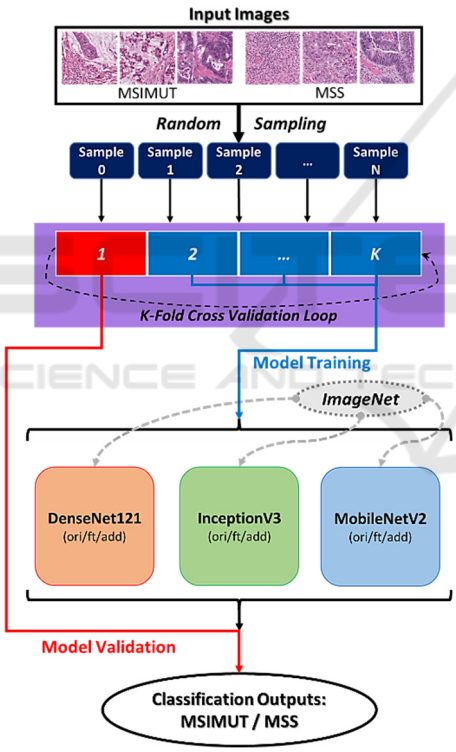

Figure 2: Overall dataflow based on K-fold cross-validation.

4 LEARNING CURVE FITTING USING INVERSE POWER LAW

For a given classification problem, fitted learning curves can be utilised for selecting models, predicting the effectiveness of using more data, as well as reducing computational complexity. Although there exist various parametric forms to fit learning curves, recent studies have shown that most deep neural networks have power law behaviour with solid empirical evidence (Viering & Loog, 2023). Therefore, similar as some previous studies (Mukherjee et al., 2003; Ali et al., 2018), the inverse power law was applied to this study:

$$IP(n) = a \times n^{-b} + c \quad (1)$$

where $a \in (-\infty, +\infty)$, $b \in (-\infty, +\infty)$ and $c \in [0, 1]$. In this equation, c represents the estimated final performance; and $n_{0.95}$ means the number of images needed to reach 95%c, which is the estimated sample size. Besides, the trust region reflective algorithm was chosen for optimisation (Voglis & Lagaris, 2004). During the optimisation process, a, b and c initial values all set to 1.

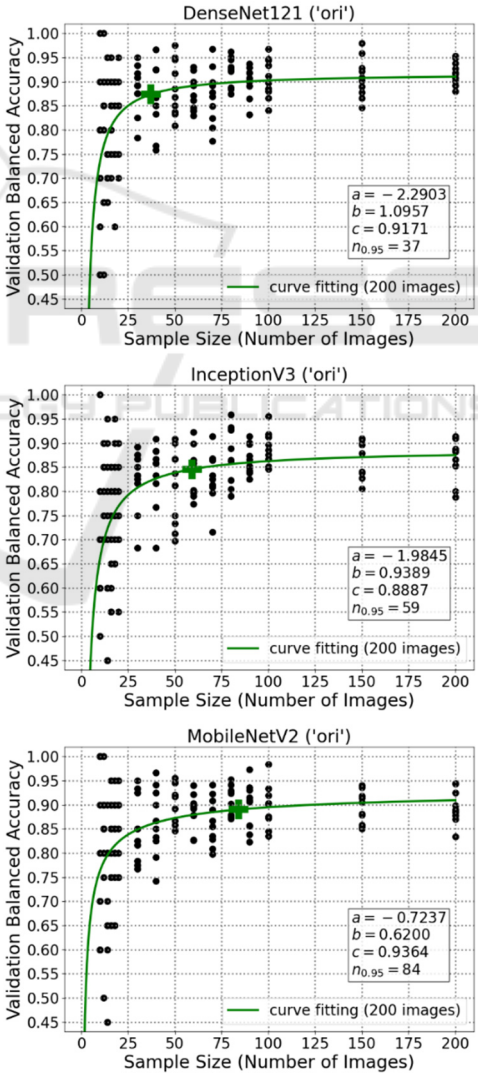

Figure 3: Curve fitting plots for original DenseNet121, InceptionV3 and MobileNetV2.

As illustrated in Figure 3, the fitted learning curves of simply using original networks ('ori') are plotted for DenseNet121, InceptionV3 and MobileNetV2, respectively. It can be found that for DenseNet121 ('ori'), the estimated final validation balanced accuracy (c) is 0.9171, and 37 images are needed to reach 95% of this performance ($n_{0.95}$). Besides, for InceptionV3 ('ori') and MobileNetV2 ('ori'), their c values are 0.8887 and 0.9364, respectively; and their $n_{0.95}$ values are 59 and 84, respectively. The plots show that simply using the original networks can have an acceptable performance when there are only limited data.

5 EXPERIMENT RESULTS WITH DIFFERENT MODEL TRANSFER METHODS

To investigate how other model transfer methods perform with limited available data, the curve fitting experiments were also conducted based on 'ft' and 'add' methods. Their results are introduced in the following.

5.1 Results Using Fine-Tuning

Firstly, the methods of fine-tuning 1 ('ft1'), 2 ('ft2') or 3 ('ft3') last layers at the end of network were applied. These results for DenseNet121 are illustrated in Figure 4. And these plots for InceptionV3 and MobileNetV2 are attached in the appendix section.

As demonstrated in the plots, DenseNet121 ('ft1') has a prediction of final performance with 0.9538 validation balanced accuracy; and it needs 119 image samples to achieve 95% of that accuracy. Besides, DenseNet121 ('ft2') needs 43 images to achieve 95% of the validation balanced accuracy 0.9063. In addition, for DenseNet121 ('ft3'), 622 images are required for 95% of a perfect predicted final performance (100%).

It is quite clear that the 'ft1' and 'ft2' could also deal well with limited number of images, but it might be challenging for the more complicated method 'ft3'. Although 'ft3' had high predicted final performance (even 100%), the required number of images is beyond the limitation of this study and too high for a medical pre-study.

5.2 Results Using Additional Convolutional Layers

Beside the aforementioned fine-tuning experiments, additional convolutional layers were also added to the

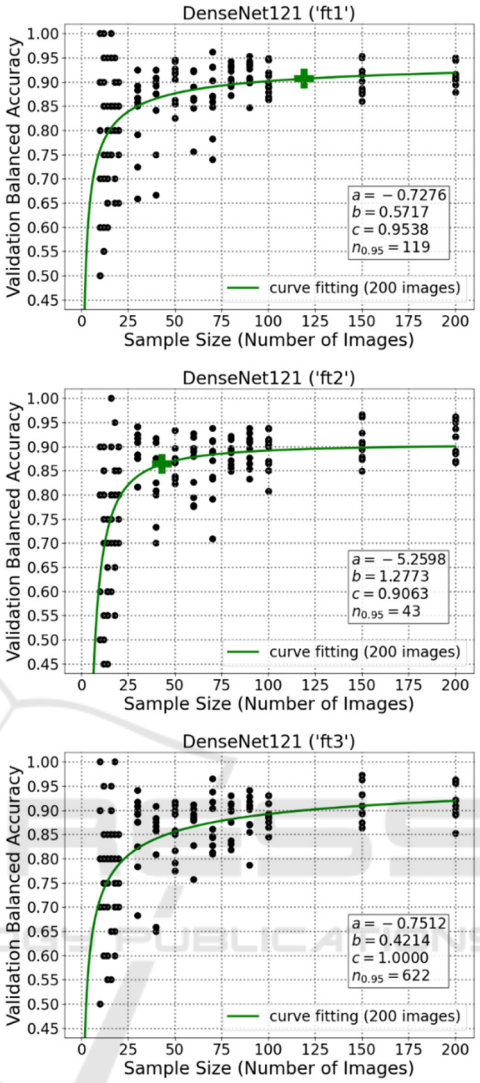

Figure 4: Curve fitting plots for DenseNet121 fine-tuning the last 1, 2, and 3 layers, respectively.

transfer learning networks for further comparison. With a kernel size of 3, 2048 filters were contained in each additional convolutional layer. And for this study, the numbers of additional convolutional layers were 1 ('add1'), 2 ('add2') or 3 ('add3'). Afterwards, learning curve fitting was also carried out in the same way as previously introduced for each model. Figure 5 consists of the curve fitting plots for DenseNet121 using 'add1', 'add2' as well as 'add3'.

From these plots, it is visible that the predicted final performance of DenseNet121 ('add1') is 0.8871, while 17 images are necessary to reach its 95%. Besides, despite DenseNet121 ('add2') and DenseNet121 ('add3') apparently have very high predicted final performance (1 and 0.9759), due to network complexity, their estimated sample size

values are both more than 3000, which could be impractical for plenty of biomedical applications.

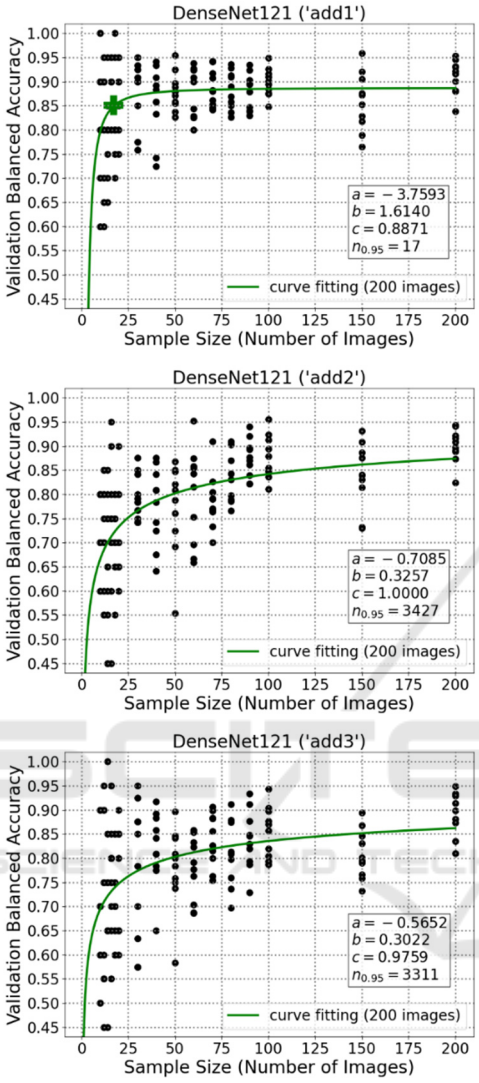

Figure 5: Curve fitting plots for DenseNet121 using 1, 2, and 3 additional convolutional layers, respectively.

5.3 Summary of Learning Curve Fitting Results

Table 1: Experiment results for DenseNet121.

	c	95%c	$n_{0.95}$
ori	0.9171	0.8712	37
ft1	0.9538	0.9061	119
ft2	0.9063	0.8610	43
ft3	1.0000	0.9500	622
add1	0.8871	0.8427	17
add2	1.0000	0.9500	3427
add3	0.9759	0.9271	3311

Table 2: Experiment results for InceptionV3.

	c	95%c	$n_{0.95}$
ori	0.8887	0.8443	59
ft1	0.8755	0.8317	37
ft2	0.8901	0.8456	63
ft3	0.8830	0.8389	49
add1	0.8601	0.8171	28
add2	0.8555	0.8127	47
add3	0.8276	0.7862	66

Table 3: Experiment results for MobileNetV2.

	c	95%c	$n_{0.95}$
ori	0.9364	0.8896	84
ft1	0.9155	0.8697	43
ft2	0.8633	0.8201	26
ft3	1.0000	0.9500	208583
add1	0.9252	0.8789	75
add2	1.0000	0.9500	13119
add3	1.0000	0.9500	12514

As shown in Tables 1-3, some methods although have very high performances, e.g. 95% of the c value, but their $n_{0.95}$ values are too high to be realistic in small scale studies. For example, the 95%c values of DenseNet121 ('add2') and MobileNetV2 ('add3') are both 0.95, but their $n_{0.95}$ values are 3427 and 12514. On the other hand, some methods just have tolerable 95%c values and their $n_{0.95}$ values are acceptable for limited available data: for example, the 95%c values of DenseNet121 ('ft1'), InceptionV3 ('ft2'), and MobileNetV2 ('ori') are 0.9061, 0.8456 and 0.8896, while their $n_{0.95}$ values are 37, 63 and 84, respectively. They outperformed the state-of-art methods using transfer learning as feature extractor with PCA-LDA and PCA-SVM (just around 0.50), 'ori' (around 0.80) and 'ft' (mostly below 0.85) even with over 9,000 images from the same dataset (Luo & Bocklitz, 2023).

Therefore, it is found that the model transfer methods for large datasets do not automatically apply to small datasets, and there is a trade-off between predicted final performance (c) and estimated sample size ($n_{0.95}$). Besides, despite of possible high final performance, complicated networks are not recommended for small datasets, while simple transfer learning methods are more practical, e.g. 'ori' and 'ft1' for all 3 networks in Tables 1-3.

6 FITTED CURVE PREDICTION

Afterwards, to investigate how many images are needed for curve fitting, the maximum number of

images changed from 200 to smaller numbers: 100, 80, 60, 40 and 20. Figure 6 shows the examples of fitted curve predictions for DenseNet121 (‘ori’), InceptionV3 (‘ori’), and MobileNetV2 (‘ori’), respectively. And the rest plots for ‘ft’ and ‘add’ model transfer methods are in the appendix. As shown in the plots, very small datasets usually lead to problematic prediction of learning curve, e.g. 20 images. Besides, at least 80 images are necessary to obtain an acceptable prediction of learning curve. Additionally, it can also be found that complicated networks still are not recommended for small datasets because of too many required images, e.g. ‘ft3’, ‘add2’, ‘add3’.

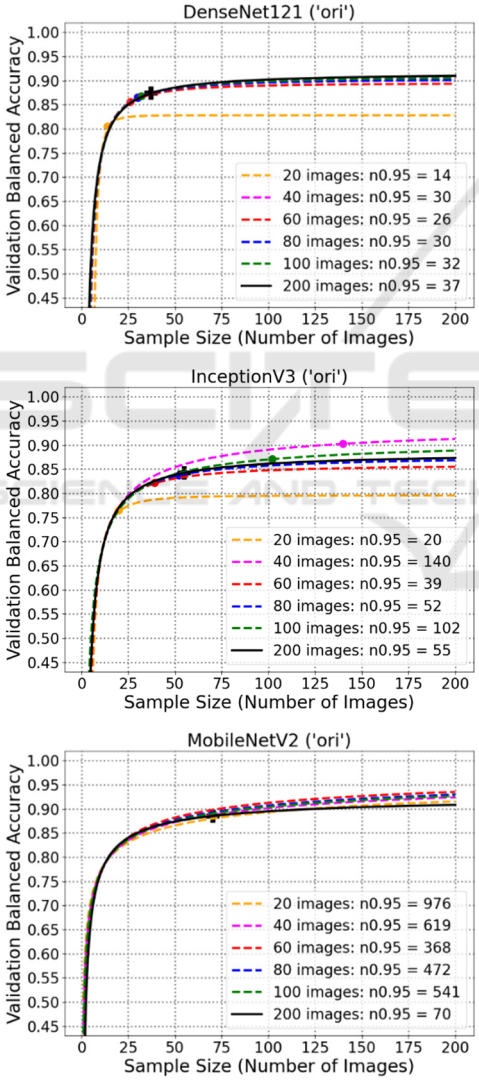

Figure 6: Plots of fitted curve prediction for original DenseNet121, InceptionV3 and MobileNetV2.

7 CONCLUSIONS

With only 200 limited images randomly chosen from a colorectal cancer dataset, this study conducted the experiments to estimate required sample sizes for satisfactory performance. In this study, three deep learning networks (DenseNet121, InceptionV3 and MobileNetV2) and different transfer methods (‘ori’, ‘ft’ and ‘add’) were compared by their validation balanced accuracies, which were generated from an external K-fold cross-validation loop. With these accuracies, learning curves were then fitted by inverse power law to obtain the values for final prediction performance (c) and the number of required images to reach of the final performance 95%c ($n_{0.95}$). Based on experiment results, well-performed model transfer methods for large datasets cannot be automatically applied to small datasets, and a trade-off has been found between predicted final performance (c) and estimated sample size ($n_{0.95}$). Besides, complicated networks are not recommended for small datasets regardless of possible high final performance, instead simple transfer learning methods are more feasible for medical applications with only limited images. Afterwards, by reducing the maximum number of images, fitted learning curves were predicted. From these experiments, it is discovered that very small datasets (e.g. 20 images) can cause seriously erroneous predictions, and at least 80 images should be contained for an acceptable prediction of learning curve. Additionally, due to model complexity and limited available data, complicated networks (e.g. ‘ft3’, ‘add2’, ‘add3’) also did not perform desirably for predicting learning curves.

Future works are planned to be done to further improve this study. For example, this study procedure is planned to be implemented to other datasets beyond colorectal cancer detection for verifying generalisability. In addition, various data augmentation techniques will be tested for their ability to improve model performance, but also for their effect on the sample size.

ACKNOWLEDGEMENTS

This work is supported by the BMBF, funding program Photonics Research Germany (13N15466 (LPI-BT1), 13N15710 (LPI-BT3)) and is integrated into the Leibniz Center for Photonics in Infection Research (LPI). The LPI initiated by Leibniz-IPHT, Leibniz-HKI, Friedrich Schiller University Jena and

Jena University Hospital is part of the BMBF national roadmap for research infrastructures. Co-funded by the European Union (ERC, STAIN-IT, 101088997). Views and opinions expressed are however those of the author(s) only and do not necessarily reflect those of the European Union or the European Research Council. Neither the European Union nor the granting authority can be held responsible for them.

REFERENCES

Ali, N., Girnus, S., Rösch, P., Popp, J., & Bocklitz, T. (2018). Sample-size planning for multivariate data: a Raman-spectroscopy-based example. *Analytical Chemistry*, *90*(21), 12485-12492. Doi: 10.1021/acs.analchem.8b02167.

Cheung, C. Y., Ran, A. R., Wang, S., Chan, V. T. T., Sham, K., Hilal, et al. (2022). A deep learning model for detection of Alzheimer's disease based on retinal photographs: a retrospective, multicentre case-control study. *Lancet Digital Health*, *4*(11), 806-815. Doi: 10.1016/S2589-7500(22)00169-8.

Cortes, C., Jackel, L. D., Solla, S. A., Vapnik, V., & Denker, J. S. (1993). Learning Curves: Asymptotic Values and Rate of Convergence. *In Proceedings of Advances in Neural Information Processing Systems 6 (NIPS 1993)*, 327-334.

Foersch, S., Glasner, C., Woerl, A. C., Eckstein, M., Wagner, D. C., Schulz, S., Kellers, F., Fernandez, A., Tserea, K., Kloth, M., Hartmann, A., Heintz, A., Weichert, W., Roth, W., Geppert, C., Kather, J. N., & Jesinghaus, M. (2023). Multistain deep learning for prediction of prognosis and therapy response in colorectal cancer. *Nature Medicine*, *29*(2), 430-439. Doi:10.1038/s41591-022-02134-1.

Huang, G., Liu, Z., van der Maaten, L., & Weinberger, K. Q. (2017). Densely connected convolutional networks. *In Proceedings of 2017 IEEE Conference on Computer Vision and Pattern Recognition (CVPR)*. 4700-4708. Doi: 10.1109/CVPR.2017.243.

Kather, J. N., Pearson, A. T., Halama, N., Jäger, D., Krause, J., Loosen, S. H., Marx, A., Boor, P., Tacke, F., Neumann, U. P., Grabsch, H. I., Yoshikawa, T., Brenner, H., Chang-Claude, J., Hoffmeister, M., Trautwein, C., & Luedde, T. (2019). Deep learning can predict microsatellite instability directly from histology in gastrointestinal cancer. *Nature Medicine*, *25*(7), 1054-1056. Doi: 10.1038/s41591-019-0462-y.

Kim, H. E., Cosa-Linan, A., Santhanam, N., Jannesari, M., Maros, M. E., & Ganslandt, T. (2022). Transfer learning for medical image classification: a literature review. *BMC Medical Imaging*, 22(1), 1-13. Doi: 10.1186/s12880-022-00793-7.

Kohavi, R. (1995). A study of cross-validation and bootstrap for accuracy estimation and model selection. *In Proceedings of the 14th International Joint Conference on Artificial Intelligence, 2,* 1137-1143.

Lecun, Y., Bengio, Y., & Hinton, G. (2015). Deep learning. *Nature* 521, 436-444. Doi:10.1038/nature14539.

Luo, R., & Bocklitz, T. (2023). A systematic study of transfer learning for colorectal cancer detection. *Informatics in Medicine Unlocked*, 40, 1-11. Doi: 10.1016/j.imu.2023.101292.

Morid, M. A., Borjali, A., & Fiol, D. G. (2021). A scoping review of transfer learning research on medical image analysis using ImageNet. *Computers in Biology and Medicine*, 128, 1-14. Doi: 10.1016/j.compbiomed.2020.104115.

Mukherjee, S., Tamayo, P., Rogers, S., Rifkin, R., Engle, A., Campbell, C., Golub, T. R., & Mesirov, J. P. (2003). Estimating dataset size requirements for classifying DNA microarray data. *Journal of Computational Biology*, 10(2), 119-142. Doi: 10.1089/10665270 3321825928.

Narayan, V., Mall, P. K., Alkhayyat, A., Abhishek, K., Kumar, S., & Pandey, P. (2023). Enhance-Net: an approach to boost the performance of deep learning model based on real-time medical images. *Journal of Sensors*, 2023, 1-15. Doi: 10.1155/2023/8276738.

Placido, D., Yuan, B., Hjaltelin, J. X., et al. (2023). A deep learning algorithm to predict risk of pancreatic cancer from disease trajectories. *Nature Medicine*, *29*(5), 1113–1122. Doi: 10.1038/s41591-023-02332-5.

Rajpurkar, P., Chen, E., Banerjee, O., & Topol, E. J. (2022). AI in health and medicine. *Nature Medicine*, 28(1), 31-38. Doi: 10.1038/s41591-021-01614-0.

Russakovsky, O., Deng, J., Su, H., Krause, J., Satheesh, S., Ma, S., Huang, Z., Karpathy, A., Khosla, A., Bernstein, M., Berg, A. C., & Fei-Fei, L. (2015). ImageNet large scale visual recognition challenge. *International Journal of Computer Vision*, *115*(3), 211-252. Doi: 10.1007/s11263-015-0816-y.

Samala, R.K., Chan, H.P., Hadjiiski, L., et al. (2019). Breast cancer diagnosis in digital breast tomosynthesis: effects of training sample size on multi-stage transfer learning using deep neural nets. *In Proceedings of the IEEE Transactions on Medical Imaging*, 38(3), 686-696. Doi: TMI.2018.2870343.

Sandler, M., Howard, A., Zhu, M., Zhmoginov, A., & Chen, L. C. (2018). MobileNetV2: inverted residuals and linear bottlenecks. *In Proceedings of the IEEE Computer Society Conference on Computer Vision and Pattern Recognition*, 4510-4520. Doi: 10.1109/CVPR.2018.00474.

Soekhoe, D., & Putten, P.V.D. (2016). On the impact of data set size in transfer learning using deep neural networks. *In Proceedings of Advances in Intelligent Data Analysis XV (IDA 2016)*, 9897, 50-60. Doi: 10.1007/978-3-319-46349-0.

Szegedy, C., Vanhoucke, V., Ioffe, et al. (2016). Rethinking the Inception architecture for computer vision. *In Proceedings of 2016 IEEE Conference on Computer Vision and Pattern Recognition (CVPR)*, 2818-2826. Doi: 10.1109/CVPR.2016.308.

Viering, T., & Loog, M. (2023). The shape of learning curves: a review. *IEEE Transactions on Pattern*

Analysis and Machine Intelligence, *45*(6), 7799-7819. Doi: 10.1109/TPAMI.2022.3220744.

Voglis, C., & Lagaris, I. E. (2004). A rectangular trust region dogleg approach for unconstrained and bound constrained nonlinear optimization. *In Proceedings of International Conference on Applied Mathematics*, 1-7.

Wang, G., Luo, X., Gu, R., et al. (2023). PyMIC: a deep learning toolkit for annotation-efficient medical image segmentation. *Computer Methods and Programs in Biomedicine*, 231, 1-11. Doi: j.cmpb.2023.107398.

Yu, X., Wang, J., Hong, Q. Q., Teku, R., Wang, S. H., & Zhang, Y. D. (2022). Transfer learning for medical images analyses: a survey. *Neurocomputing*, *489*, 230-254. Doi: 10.1016/j.neucom.2021.08.159.

Zhuang, F., Qi, Z., Duan, et al. (2021). A comprehensive survey on transfer learning. *Proceedings of the IEEE* 109(1), 43-76. Doi: 10.1109/JPROC.2020.3004555.

Zhu, W., Braun, B., Chiang, L. H., & Romagnoli, J. A. (2021). Investigation of transfer learning for image classification and impact on training sample size. *Chemometrics and Intelligent Laboratory Systems*, 211, 1-9. Doi: 10.1016/j.chemolab.2021.104269.

APPENDIX

A: Plots of Learning Curve Fitting Using Fine-Tuning for InceptionV3 and MobileNetV2

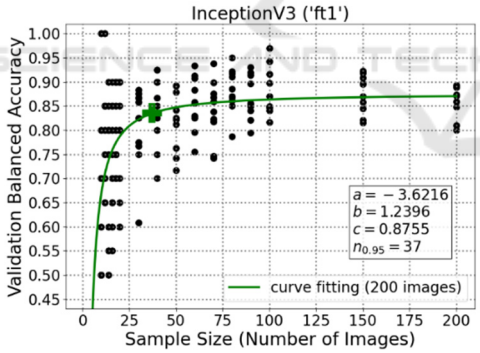

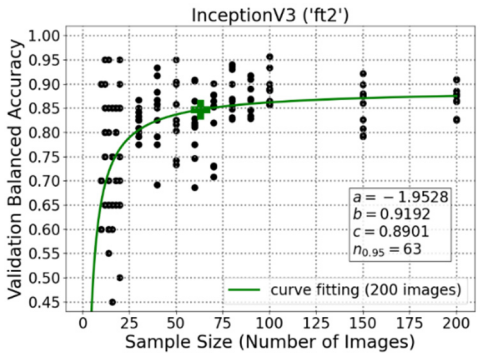

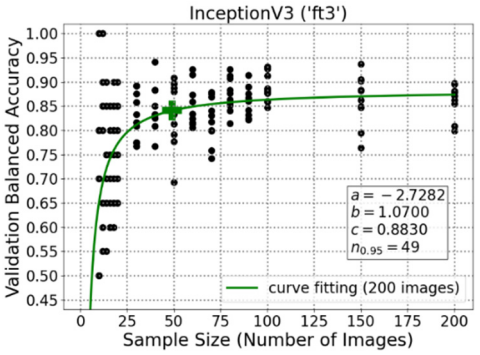

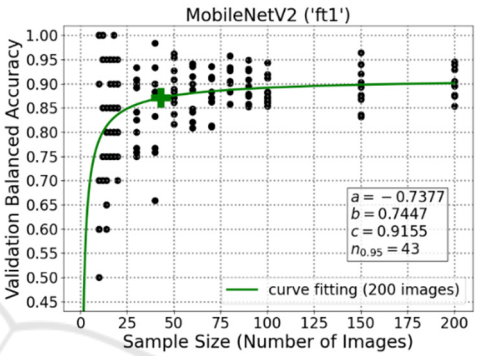

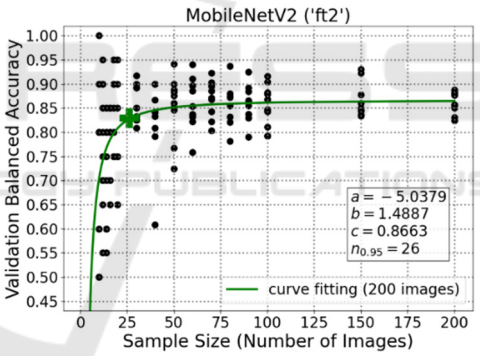

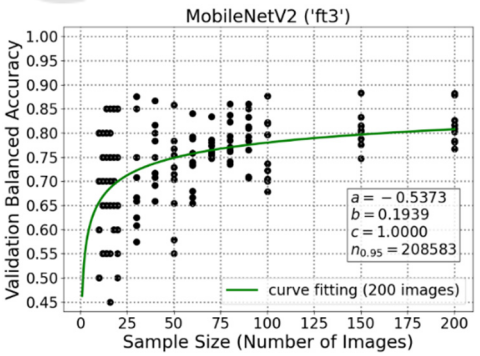

B: Plots of Learning Curve Fitting Using Additional Convolutional Layers for InceptionV3 and MobileNetV2

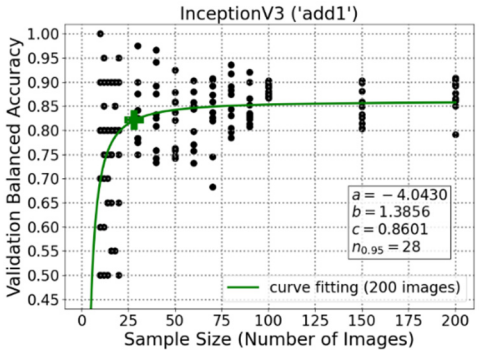

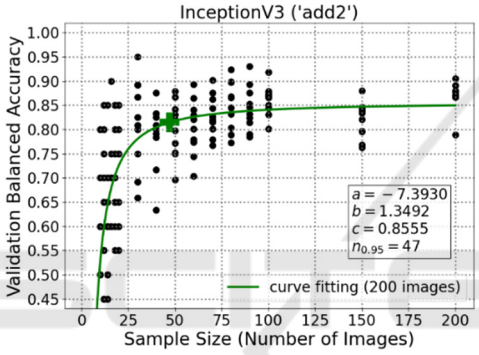

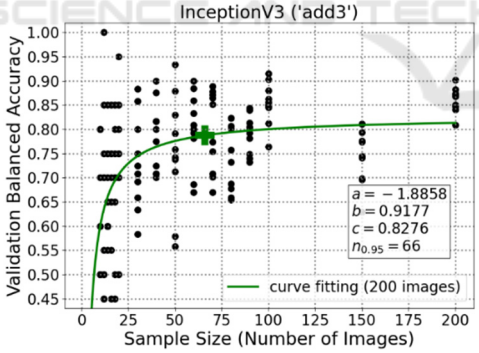

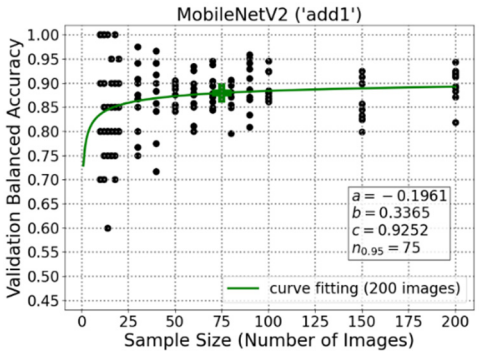

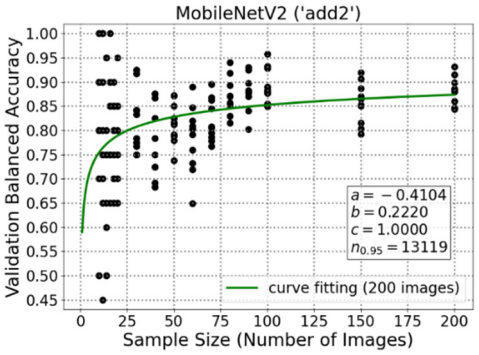

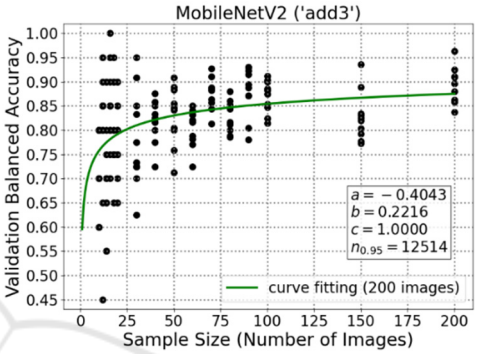

C: Plots of Fitted Curve Prediction Using Fine-Tuning

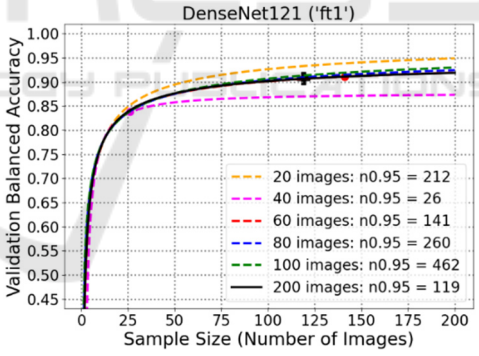

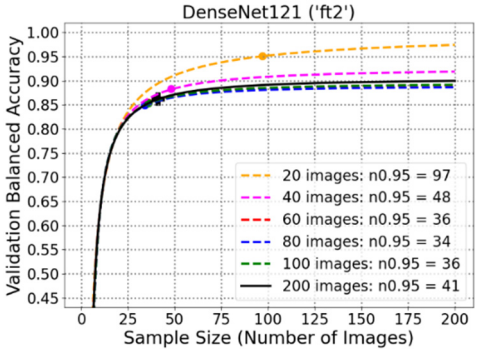

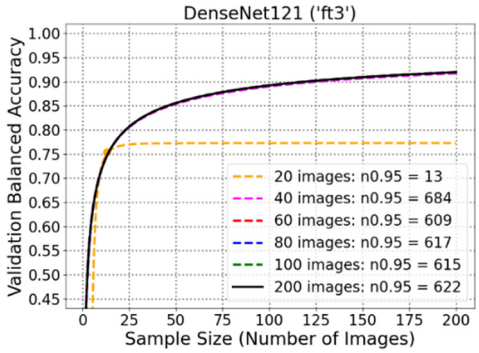

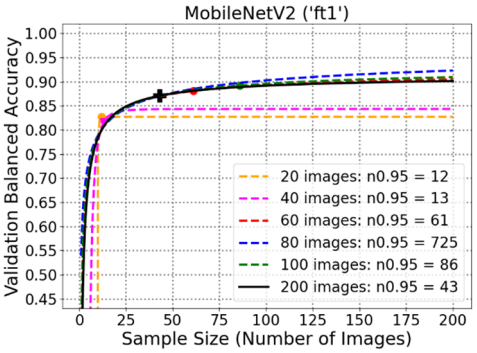

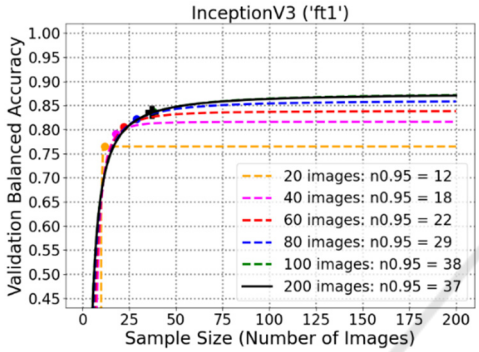

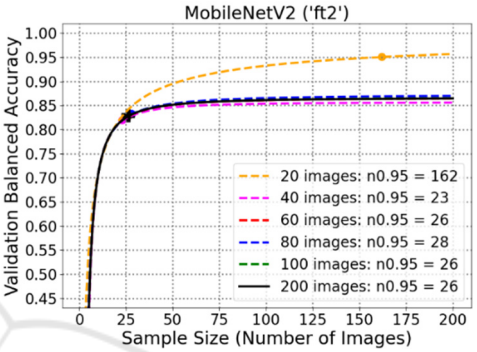

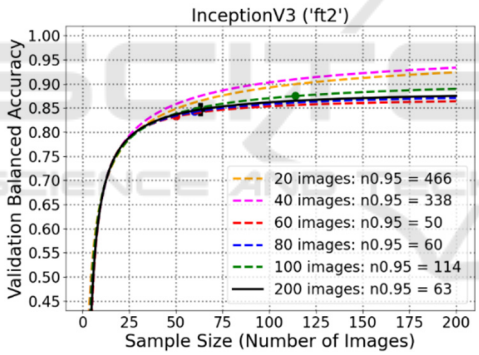

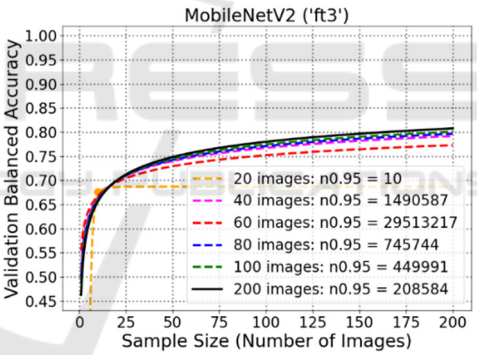

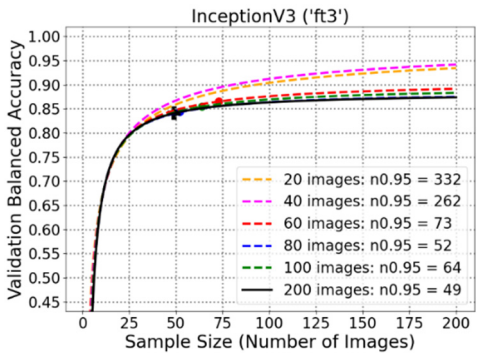

D: Plots of Fitted Curve Prediction Using Additional Convolutional Layers

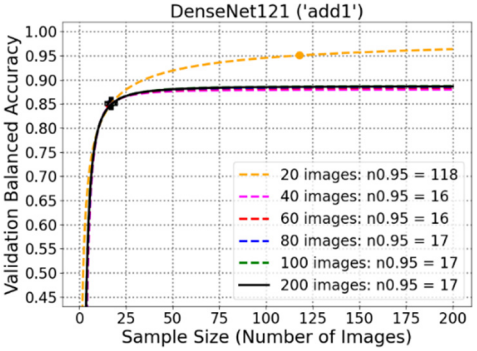

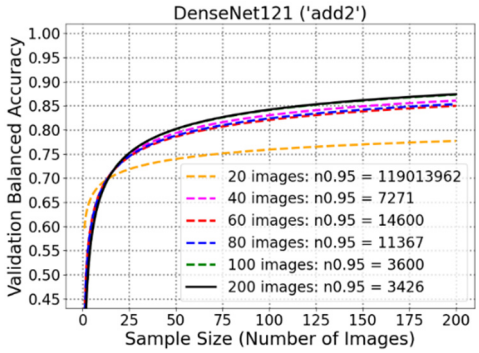
DenseNet121 ('add2')
Validation Balanced Accuracy
Sample Size (Number of Images)
20 images: n0.95 = 119013962
40 images: n0.95 = 7271
60 images: n0.95 = 14600
80 images: n0.95 = 11367
100 images: n0.95 = 3600
200 images: n0.95 = 3426

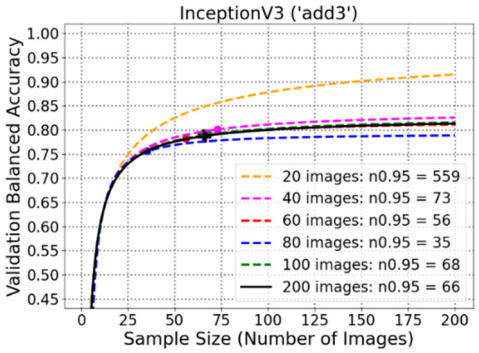
InceptionV3 ('add3')
Validation Balanced Accuracy
Sample Size (Number of Images)
20 images: n0.95 = 559
40 images: n0.95 = 73
60 images: n0.95 = 56
80 images: n0.95 = 35
100 images: n0.95 = 68
200 images: n0.95 = 66

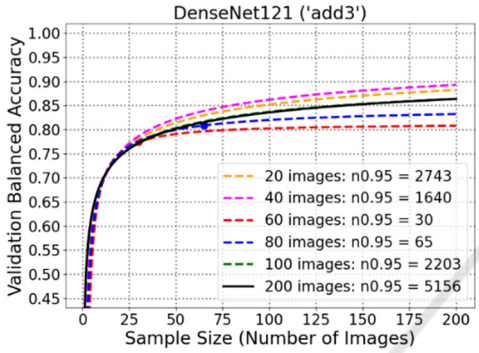
DenseNet121 ('add3')
Validation Balanced Accuracy
Sample Size (Number of Images)
20 images: n0.95 = 2743
40 images: n0.95 = 1640
60 images: n0.95 = 30
80 images: n0.95 = 65
100 images: n0.95 = 2203
200 images: n0.95 = 5156

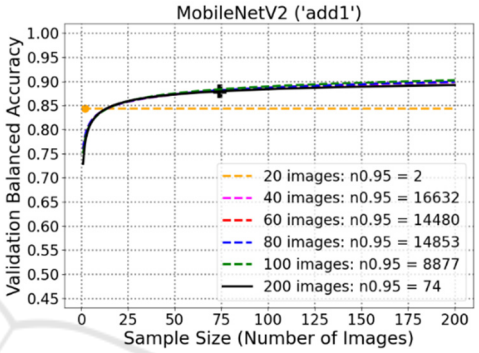
MobileNetV2 ('add1')
Validation Balanced Accuracy
Sample Size (Number of Images)
20 images: n0.95 = 2
40 images: n0.95 = 16632
60 images: n0.95 = 14480
80 images: n0.95 = 14853
100 images: n0.95 = 8877
200 images: n0.95 = 74

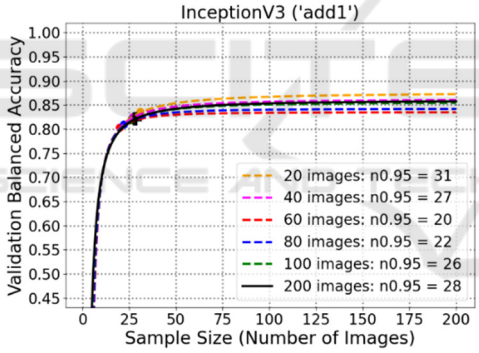
InceptionV3 ('add1')
Validation Balanced Accuracy
Sample Size (Number of Images)
20 images: n0.95 = 31
40 images: n0.95 = 27
60 images: n0.95 = 20
80 images: n0.95 = 22
100 images: n0.95 = 26
200 images: n0.95 = 28

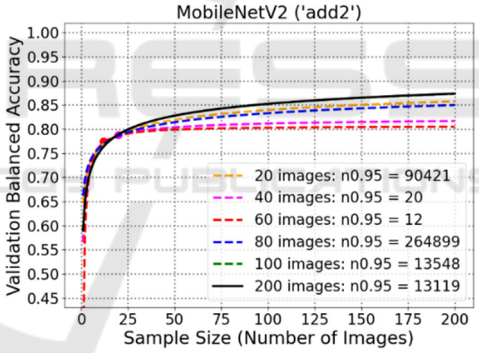
MobileNetV2 ('add2')
Validation Balanced Accuracy
Sample Size (Number of Images)
20 images: n0.95 = 90421
40 images: n0.95 = 20
60 images: n0.95 = 12
80 images: n0.95 = 264899
100 images: n0.95 = 13548
200 images: n0.95 = 13119

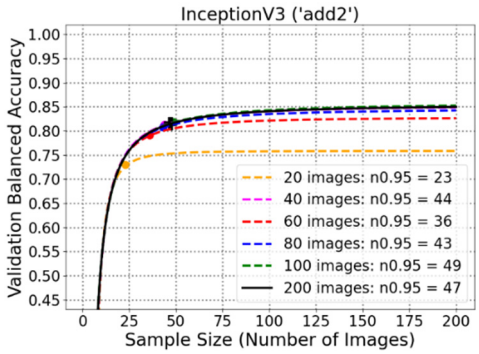
InceptionV3 ('add2')
Validation Balanced Accuracy
Sample Size (Number of Images)
20 images: n0.95 = 23
40 images: n0.95 = 44
60 images: n0.95 = 36
80 images: n0.95 = 43
100 images: n0.95 = 49
200 images: n0.95 = 47

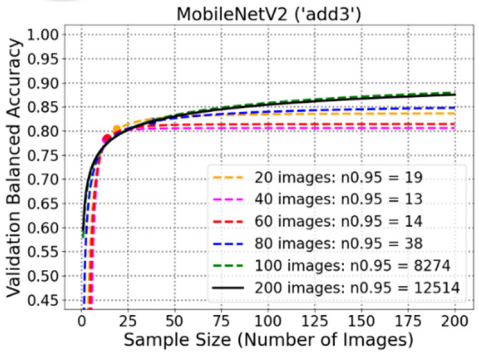
MobileNetV2 ('add3')
Validation Balanced Accuracy
Sample Size (Number of Images)
20 images: n0.95 = 19
40 images: n0.95 = 13
60 images: n0.95 = 14
80 images: n0.95 = 38
100 images: n0.95 = 8274
200 images: n0.95 = 12514